Compressive ion acoustic double layer and its transitional properties for a two electron temperature warm, multi-ion plasma

S. V. Steffy[a)] and S. S. Ghosh[b)]
Indian Institute of Geomagnetism, Navi Mumbai, India

The emergence of the compressive ion acoustic double layer has been investigated for a two electron temperature warm, multi-ion plasma by the Sagdeev pseudopotential technique. It shows that the ambient cooler electron concentration plays a deterministic role in initiating the transition process of a compressive ion acoustic solitary wave to its double layer. Incorporating the derivative analysis for the pseudopotential, the transitional phase was further quantified by assigning a critical value for the ambient cooler electron concentration. It has been observed that, beyond that critical value, the width of the solitary wave increases rapidly with the increasing amplitude which coincides with the aforementioned transitional phase, manifesting a change in the internal microphysics of the structure for that region. A comparison with the satellite observation revealed good agreement validating the present model. The model will be useful in interpreting the observed monopolar structures in the auroral acceleration region. *Published by AIP Publishing.* https://doi.org/10.1063/1.5006972

I. INTRODUCTION

Plasma, being a highly nonlinear medium, is one of the convenient test beds to study different nonlinear wave structures. Localized nonlinear structures, such as Solitary Waves (SWs) and Double Layers (DLs), arise due to the balance between the nonlinearity of the wave and the dispersion, or the dissipation, of the wave in the medium. Among different plasma systems, space plasma is an excellent laboratory for the investigation of nonlinear localized structures. Satellite observations have revealed bipolar and monopolar electric field pulses at different regions of the magnetospheric boundary layers.[1–3] Slow moving bipolar electric field pulses in the auroral region[4] are often interpreted as Ion Acoustic Solitary Waves (IASWs), whereas a corresponding monopolar pulse associated with an ion beam is generally interpreted as an ion acoustic Weak Double Layer (WDL).[5]

The subject DL has attracted great attention since Alfvén and Carlqvist, who have suggested the current disruption theory of solar flares.[6] A DL is a localized structure in the plasma which consists of two parallel layers with opposite electrical charges. They can effectively accelerate or decelerate charged particles, dissipate energy, and cause a local break in the frozen condition. Due to these properties, they have attracted a great deal of attention in the space plasma-related studies. DLs occur naturally in various space plasma environments, like the aurora,[7] the plasmasheet,[8] the solar wind,[9] or other magnetospheric boundary layers.[10,11] The first space observation of DL was reported by Temerin *et al.*[7] along the auroral field lines. This is followed by several other direct observational evidences of DLs in the auroral acceleration region.[12–14] The observational evidences of the auroral region proves that the DL occurs naturally in regions which are highly kinetic by non-ideal processes. Later, Ergun *et al.*[8] reported the first direct observation

of DLs in the Earth's plasma sheet which lies well outside the auroral acceleration region. Besides satellite observations,[7,8,12,14] ion acoustic DLs have been studied extensively in the theory[15–17] and laboratory experiments[18,19] as well as by numerical simulations.[20–22] Several numerical simulations have pointed out that an ion acoustic DL can be formed by the reflection of electrons off the negative potential depressions.[23–26] In other words, majority of the theoretical works found that an ion acoustic DL is, in general, closely associated with the corresponding rarefactive (negative amplitude) IASW. Assuming a fluid model, ion acoustic DLs have been obtained for both an weakly nonlinear analysis[27–29] as well as from the Sagdeev pseudopotential formalism where the latter may also encompass large amplitude solutions.[30,31] A kinetic mode DL, on the other hand, is often related to the phase space density hole.[16,32,33]

According to the previous analyses, it is well established that the existence domain of a rarefactive (negative amplitude) IASW terminates with a corresponding DL solution whereas that for the compressive (positive amplitude) one terminates due to the steepening and wave breaking. Although there have been many theoretical and numerical investigations of rarefactive ion acoustic DLs, studies related to a compressive ion acoustic DL have comparatively received scant attention so far. In its first observational evidence, Temerin *et al.*[7] have interpreted the monopolar electric field pulses as DLs of both the positive (i.e., compressive), as well as the negative (rarefactive) polarities. They argued that the rarefactive DLs are moving upward from the ionosphere to the magnetosphere, whereas the compressive DLs are moving downward from the magnetosphere to the ionosphere. It is also noticed that the compressive DL, moving downward, damps out very quickly due to the insufficient concentration of negative ions. Later Goswami and Bujarbarua[28] interpreted the observation of Temerin *et al.*[7] by adopting the weakly nonlinear theory. They obtained compressive ion acoustic DLs with a positive potential in the presence of negative ions. They also studied the plasma system comprising of cold ions and two electron

a)Electronic mail: steffystephan28@gmail.com
b)Electronic mail: sukti@iigs.iigm.res.in

species, each with a distinct Maxwellian distribution, and obtained both compressive and rarefactive ion acoustic DLs. They were the first to infer that there is no DL for a two component plasma system with a single species of Maxwellian electrons.[27] There are many examples in literature for rarefactive DLs for a two electron temperature electrons, or negative ions. In most of the cases, both of the electrons were assumed to obey the Boltzmann distribution separately in thermal equilibrium. Roychoudhury and Bhattacharya[30] studied small amplitude DLs in a magnetized plasma comprising of two electron temperatures and cold ions. Adopting Sagdeev pseudopotential technique and without assuming a quasi-neutrality condition, they showed that the DL solution obtained by using Poisson's equation is significantly different from those obtained from the quasi-neutrality condition. Their analytical and numerical solutions show both compressive and rarefactive ion acoustic DLs. Shortly after them, Baboolal *et al.*[34] obtained arbitrary amplitude solutions for rarefactive DLs in an unmagnetized plasma where they claimed that their solutions were confined only to the rarefactive solitary waves of negative polarity. On the other hand, using reductive perturbation method, Tagare[29] obtained both rarefactive and compressive ion acoustic DLs where he deduced the conditions for the respective polarities based on the concentration of the cooler electrons. Later Verheest *et al.*[31] quantified the findings of Baboolal *et al.*[34] and showed that it is also possible to obtain a compressive DL for their model, but those solutions are confined only to a narrow domain with marginally super-ion-acoustic flows. Compressive ion acoustic DLs have also been obtained in plasma system containing positrons.[35,36] Ghosh and Iyengar[37] obtained both compressive ion acoustic DLs and Super Solitary Waves (SSWs) in a three component plasma comprising of two electron temperatures obeying Boltzmann distributions and warm ions. They have shown that it is the electron temperature ratio which determines the parameter regime supporting the DL.

It is well known that a rarefactive IASW, ubiquitously, terminates to a DL. Ghosh and Iyengar,[37] however, have shown that, depending on the parameter regime, the termination process of the compressive solitary wave may differ and thus may give rise to a compressive DL. Although there exists an extensive theoretical analysis of a rarefactive IASW and DLs, the particular transition process through which a rarefactive solitary wave transforms to the terminating solution of DL has received a lesser attention so far. Even fewer attempts have been made to analyze its positive amplitude analogue

where a compressive ion acoustic DL emerges out of the ion acoustic solitary wave with the same polarity. The relative lacuna motivated us to revisit the onset of the compressive DL and its correlation with the corresponding solitary wave. In our recent works,[38,39] we have successfully incorporated a derivative analysis to classify different nonlinear structures where, in spite of their finer differences, they all follow the same boundary conditions [Eq. (4)] and thus fall within the ambit of the generalized solitary wave solutions. The derivative analysis further enabled us to understand the particular steps through which a Regular Solitary Wave (RSW) may transform to an SSW. These correlations also helped us to determine the parametric conditions and the existence domain of the SSW. In the present paper, we continued with the same plasma model but focussed our attention to that parameter regime where the terminating solutions are compressive DLs. Our analyses reveal that the cooler electron concentration plays a deterministic role in the transition of the compressive RSW to its DL. This further reveals that, for this particular parameter regime, there is a kind of "degeneracy" in the otherwise RSW solutions. Depending on a critical value of the cooler electron concentration, the derivative profiles, the charge separation, and the width-amplitude variation profiles differ significantly. A comparison with the satellite observation further indicates that our theoretical estimations may be relevant in interpreting the observed monopolar pulses in the auroral region.

This paper is organized as follows: Section II presents the analytical form of the Sagdeev pseudopotential (Sec. II A) and its derivatives (Sec. II B) for a two electron temperature warm multi-ion plasma, while Sec. III presents the analysis of the corresponding RSW and DL solutions. In Sec. III A, we have discussed and validated the derivative analysis described by Varghese and Ghosh,[38] while in Sec. III B, we have analyzed the width-amplitude variation of the nonlinear structures for the selected parametric regime. In Sec. III C, we have validated the model with observational data. The exact existence domains for both the compressive solitary waves and DLs have been delineated for our model in Sec. III D assuming a chosen set of parameters, and Sec. IV presents the conclusion.

II. FORMULATION

A. Sagdeev pseudopotential analysis

The plasma is assumed to be infinite, homogeneous, collisionless, and unmagnetised. The Sagdeev pseudopotential for two electron temperature warm multi-ion plasma is given as[38]

$$\Psi(\Phi) = -\left[(\mu+\nu\beta)\left(\mu\left(\exp\frac{\Phi}{\mu+\nu\beta}-1\right) + \frac{\nu}{\beta}\left(\exp\frac{\beta\Phi}{\mu+\nu\beta}-1\right) \right) \right.$$
$$+ \frac{\alpha_l}{6\sqrt{3\sigma_l}}\left(\left[\left(M+\sqrt{3\sigma_l}\right)^2-2\Phi\right]^{\frac{3}{2}} - \left(M+\sqrt{3\sigma_l}\right)^3 - \left[\left(M-\sqrt{3\sigma_l}\right)^2-2\Phi\right]^{\frac{3}{2}} + \left(M-\sqrt{3\sigma_l}\right)^3 \right)$$
$$\left. + \frac{\alpha_h}{6\sqrt{3\sigma_h}}\left(\left[\left(\frac{M}{\sqrt{Q}}+\sqrt{3\sigma_h}\right)^2-2\Phi\right]^{\frac{3}{2}} - \left(\frac{M}{\sqrt{Q}}+\sqrt{3\sigma_h}\right)^3 - \left[\left(\frac{M}{\sqrt{Q}}-\sqrt{3\sigma_h}\right)^2-2\Phi\right]^{\frac{3}{2}} + \left(\frac{M}{\sqrt{Q}}-\sqrt{3\sigma_h}\right)^3 \right) \right], \quad (1)$$

which is derived from the following warm ion densities:

$$n_{il} = \frac{\alpha_l}{2\sqrt{3\sigma_l}} \left[\left(\left(M + \sqrt{3\sigma_l}\right)^2 - 2\Phi \right)^{\frac{1}{2}} \right.$$
$$\left. - \left(\left(M - \sqrt{(3\sigma_l)}\right)^2 - 2\Phi \right)^{\frac{1}{2}} \right], \tag{2}$$

$$n_{ih} = \frac{\alpha_h}{2\sqrt{3\sigma_h}} \left[\left(\left(\frac{M}{\sqrt{Q}} + \sqrt{3\sigma_h}\right)^2 - 2\Phi \right)^{\frac{1}{2}} \right.$$
$$\left. - \left(\left(\frac{M}{\sqrt{Q}} - \sqrt{3\sigma_h}\right)^2 - 2\Phi \right)^{\frac{1}{2}} \right], \tag{3}$$

and the total electrons density is given as

$$n_e = n_{ec} + n_{ew} = \mu e^{\frac{\Phi}{\mu+\nu\beta}} + \nu e^{\frac{\beta\Phi}{\mu+\nu\beta}}, \tag{4}$$

where the subscripts i, e, l, h, c, and w represent ions, electrons, lighter and heavier ions, and cooler and warmer electrons, respectively. M is the wave Mach number, Q $\left(= \frac{m_{il}}{m_{ih}}\right)$ is the lighter to heavier ion mass ratio, where m_{il} (m_{ih}) are the mass of lighter (heavier) ions, respectively, and $\beta \left(= \frac{T_{ec}}{T_{ew}}\right)$ refers to the cooler to warmer electron temperature ratio. The normalized ion temperatures $\sigma_j \left(= \frac{T_j}{T_{eff}}\right)$ are normalized by the effective electron temperature $T_{eff} \left(= \frac{T_{ec}T_{ew}}{\mu T_{ew} + \nu T_{ec}}\right)$, where T_j is the ion temperature, j=l and h, and $T_{ew,ec}$ are the temperatures of warmer and cooler electrons, respectively. All number densities are normalized by the total equilibrium ion density $n_0 (= n_{il} + n_{ih})$ which results in the ambient densities α_l (α_h), and μ (ν), corresponding to lighter (heavier ions) and cooler (warmer) electrons, respectively. The velocities, time, and length are normalized by the lighter ion acoustic speed $c_{isl} \sim \left(= \sqrt{\left(\frac{T_{eff}}{m_{il}}\right)}\right)$, inverse of the ion plasma frequency $\omega_{pil}^{-1} \left(= \left(\frac{n_0 e^2}{\epsilon_0 m_{il}}\right)^{-\frac{1}{2}}\right)$, and the effective Debye length $\lambda_{eff} \left(= \left(\frac{\epsilon_0 T_{eff}}{n_0 e^2}\right)^{\frac{1}{2}}\right)$, respectively. The pressure p_{ij} is normalized by the ion equilibrium pressure $p_0 (= n_0 T_i)$ and potential Φ by $\frac{T_{eff}}{e}$.

B. Derivatives of Sagdeev pseudopotential

According to the Sagdeev pseudopotential analysis

$$\frac{\partial^2 \Phi}{\partial \eta^2} = n_i - n_e = -\frac{\partial \Psi(\Phi)}{\partial \Phi}, \tag{5}$$

which leads to the energy equation

$$\frac{1}{2}\left(\frac{\partial \Phi}{\partial \eta}\right)^2 + \Psi(\Phi) = 0. \tag{6}$$

Using Eqs. (2)–(4) in Eq. (5), the first order derivative of the Sagdeev pseudopotential is given as

$$\frac{\partial \Psi(\Phi)}{\partial \Phi} = \mu \left[exp^{\left(\frac{\Phi}{\mu+\nu\beta}\right)} \right] + \nu \left[exp^{\left(\frac{\beta\Phi}{\mu+\nu\beta}\right)} \right]$$
$$- \frac{\alpha_l}{2\sqrt{3\sigma_l}} \left[\left((M + \sqrt{3\sigma_l})^2 - 2\Phi \right)^{\frac{1}{2}} \right.$$
$$\left. - \left((M - \sqrt{(3\sigma_l)})^2 - 2\Phi \right)^{\frac{1}{2}} \right]$$
$$- \frac{\alpha_h}{2\sqrt{3\sigma_h}} \left[\left(\left(\frac{M}{\sqrt{Q}} + \sqrt{3\sigma_h}\right)^2 - 2\Phi \right)^{\frac{1}{2}} \right.$$
$$\left. - \left(\left(\frac{M}{\sqrt{Q}} - \sqrt{3\sigma_h}\right)^2 - 2\Phi \right)^{\frac{1}{2}} \right], \tag{7}$$

which is equivalent to the charge separation $\Delta n (= n_i - n_e)$. Taking the derivative of Eq. (7) with Φ, the 2nd order derivative of the Sagdeev pseudopotential becomes

$$\frac{\partial^2 \Psi}{\partial \Phi^2} = -\left[\frac{1}{(\mu+\nu\beta)}\left(\mu \exp\frac{\Phi}{(\mu+\nu\beta)} + \nu\beta \exp\frac{\beta\Phi}{(\mu+\nu\beta)}\right) \right.$$
$$+ \frac{\alpha_l}{2\sqrt{(3\sigma_l)}} \left\{ \left(\left[M + \sqrt{(3\sigma_l)}\right]^2 - 2\Phi\right)^{-\frac{1}{2}} \right.$$
$$\left. - \left(\left[M - \sqrt{3\sigma_l}\right]^2 - 2\Phi\right)^{-\frac{1}{2}}\right\}$$
$$+ \frac{\alpha_h}{2\sqrt{3\sigma_h}} \left\{ \left(\left[\frac{M}{\sqrt{Q}} + \sqrt{3\sigma_h}\right]^2 - 2\Phi\right)^{-\frac{1}{2}} \right.$$
$$\left. \left. - \left(\left[\frac{M}{\sqrt{Q}} - \sqrt{3\sigma_h}\right]^2 - 2\Phi)^{-\frac{1}{2}}\right)\right\}\right], \tag{8}$$

while the 3rd order derivative of the Sagdeev pseudopotential is given as

$$\frac{\partial^3 \Psi}{\partial \Phi^3} = -\left[\frac{1}{(\mu+\nu\beta)^2}\left[\mu \exp\left(\frac{\Phi}{(\mu+\nu\beta)}\right) + \nu\beta^2 \exp\left(\frac{\beta\Phi}{(\mu+\nu\beta)}\right)\right] \right.$$
$$+ \frac{\alpha_l}{2\sqrt{3\sigma_l}} \left\{ \left(\left[M + \sqrt{3\sigma_l}\right]^2 - 2\Phi\right)^{-\frac{3}{2}} - \left(\left[M - \sqrt{3\sigma_l}\right]^2 - 2\Phi\right)^{-\frac{3}{2}}\right\}$$
$$\left. + \frac{\alpha_h}{2\sqrt{3\sigma_h}} \left\{ \left(\left[\frac{M}{\sqrt{Q}} + \sqrt{3\sigma_h}\right]^2 - 2\Phi\right)^{-\frac{3}{2}} - \left(\left[\frac{M}{\sqrt{Q}} - \sqrt{3\sigma_h}\right]^2 - 2\Phi\right)^{-\frac{3}{2}}\right\}\right]. \tag{9}$$

In order to obtain the solitary wave solution, and to ensure the recurrence of the initial state, $\Psi(\Phi)$ of Eq. (1) must satisfy the following boundary conditions:

$$\Psi(\Phi = 0) = \frac{\partial\Psi}{\partial\Phi}\bigg|_0 = 0; \quad \frac{\partial^2\Psi(0)}{\partial\Phi^2} < 0;$$

$$\Psi(\Phi_0) = 0; \quad \frac{\partial\Psi(\Phi_0)}{\partial\Phi} \neq 0. \tag{10}$$

This also implies that $\Psi(\Phi) < 0$ for $0 < \Phi < \Phi_0$, where Φ_0 is the amplitude of the solitary waves.

For an ion acoustic DL, there is no recurrence of the initial state. The last boundary condition of Eq. (11) thus modifies to the following:

$$\Psi(\Phi_d) = 0; \quad \frac{\partial\Psi(\Phi_d)}{\partial\Phi} = \Delta n_d = 0, \tag{11}$$

where Φ_d is the amplitude of the ion acoustic DL and Δn_d is the charge separation at Φ_d.

III. RESULT AND DISCUSSION

A. Derivative anlaysis

While their rarefactive counterpart is well known and well studied, the compressive ion acoustic DLs are relatively lesser known to the community. Ghosh and Iyengar[37] have previously identified forbidden regions in μ which do not support any SW solution. They have also reported that the plasma may support compressive DLs or SSWs in the low β–low μ regime associated with the forbidden region. According to their nomenclature, the regions supporting the SSW, or DL, were termed as Region B1, and B2, respectively, while Region A governs the familiar compressive

IASWs which are well known and well studied by others.[40,41] Incidentally, Region B2 belongs to the lowest part of β and μ, while Region A has large values for either of them. In our previous analyses,[38,39] we focused on Region B1 and delineated the existence domain and the transformation processes of the SSW. There, we classified RSWs and other nonlinear structures in plasma on the basis of our derivative analysis[38,39] and also could identify the intricate processes by which the former may transform to an SSW, or other extra-nonlinear structures. In the present work, we have shifted our attention to Region B2 which comprises of both the RSWs and DLs, and delineated the regime using a similar technique.

The existence domains for RSWs are well known and well studied across different plasma models[37–39] but little is known so far about its transition process to a terminating DL solution. Here, we specifically intend to analyze the transition processes of the compressive RSW to the corresponding DL on the basis of our derivative analysis. We are continuing with our previous plasma model comprising of two electron temperatures and warm multi-ions. It is assumed that the plasma is mainly comprised of H^+ ions with a minority component of He^+, having the mass ratio $Q = 1/4$ and the lighter ion concentration $\alpha_l = 0.9$. For the sake of our convenience, we choose $\sigma = 0.033$ to be the temperature of both the heavier and lighter ions, i.e., $\sigma_l = \sigma_h = \sigma$. We have further assumed that all these parameters, viz., Q, α_l, and σ, remain constant throughout our analyses.

Apart from the aforementioned parameters, we have also chosen a constant Mach number $M = 1.06$, and the electron temperature ratio is chosen as $\beta = 0.04$. Both the parameters remain constant unless specified otherwise. We have selected four convenient values of μ, the cooler
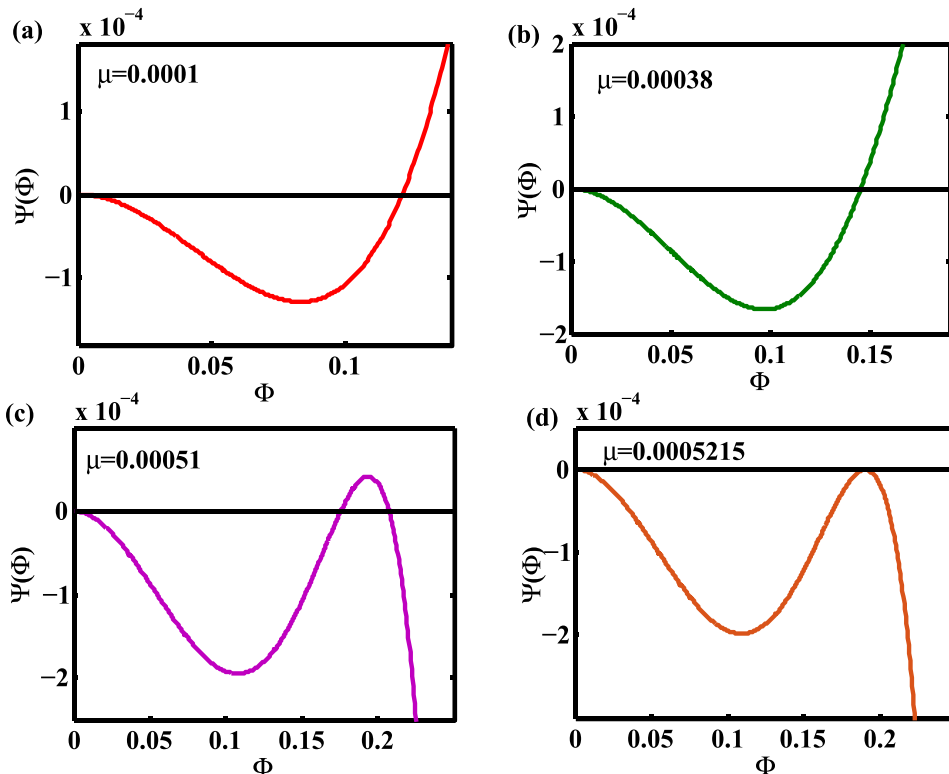
FIG. 1. Sagdeev pseudopotential profiles; curves (a) and (b) RSW, (c) transitional RSW, and (d) DL.

electron concentration, for our analysis. Figures 1(a)–1(d) show the four snapshots of the Sagdeev pseudopotentials for the chosen μ values. The first three figures [Figs. 1(a)–1(c)] represent RSWs, whereas the last one [Fig. 1(d)] represents a DL. The characteristic μ value that corresponds to a DL is represented as "μ_d." All the Sagdeev pseudopotential profiles in Figs. 1(a)–1(d) have one local extrema excluding the end points. For Figs. 1(a)–1(c), however, it crosses the zero axis, ensuring the recurrence of the initial state [Eq. (10)], while in Fig. 1(d), the profile tends to the maximum amplitude where the solution approaches another state asymptotically [Eq. (11)].

As part of the derivative analysis, we have plotted the 1st derivatives of the Sagdeev pseudopotentials $\left(\frac{\partial \Psi}{\partial \Phi}\right)$ [Eq. (7)] in Fig. 2 where the curves 1–4 represent the derivatives of the corresponding Sagdeev pseudopotential profiles shown in Figs. 1(a)–1(d), respectively. Noting the importance of the 1st derivative of the Sagdeev pseudopotential (i.e., $\frac{\partial \Psi}{\partial \Phi}$) and remembering that it represents the charge separation density (Δn),[38] we inspected all the four profiles closely. It immediately reveals two groups. The 1st group consists of curves 1 and 2, which show only one minima and beyond that Δn increases monotonically. Contrary to that, the 2nd group, i.e., curves 3 and 4, show an additional maxima revealing a decreasing trend for Δn near the maximum amplitude. This makes their variation non-monotonic which differs from the previous variation pattern. For curve 4, which corresponds to a DL, Δn vanishes at its amplitude Φ_d and recovers its initial value, i.e., $\Delta n = 0$ at $\Phi = 0$ and Φ_d. Figure 2 thus reveals a complete "bipolar" profile of Δn for curve 4. For curve 3, however, the "bipolar" variation pattern for Δn remains incomplete and the solution terminates at a decreased, but positive Δn. To summarize, initially curve 3 follows the same variation pattern as curves 1 and 2 up to a maximum value of Δn. After that, it transforms to that for curve 4 but is cut short due to the energy condition, while Δn remains positive and nonzero at Φ_0.

In order to understand the variation in the property of curve 3 from that of curves 1 and 2, where all the three
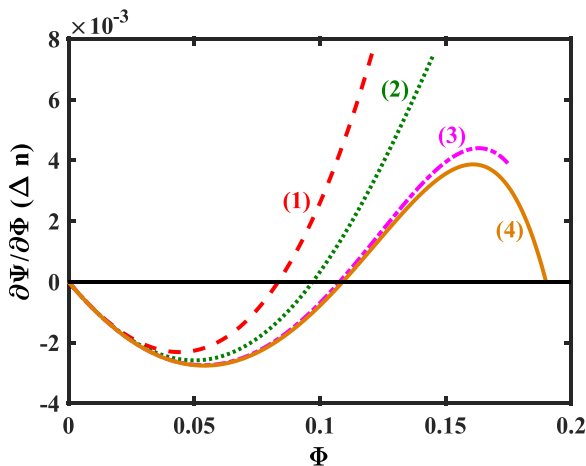
FIG. 2. Variation of Δn Vs Φ; curves (1) and (2) RSW, (3) transitional RSW, and (4) DL.
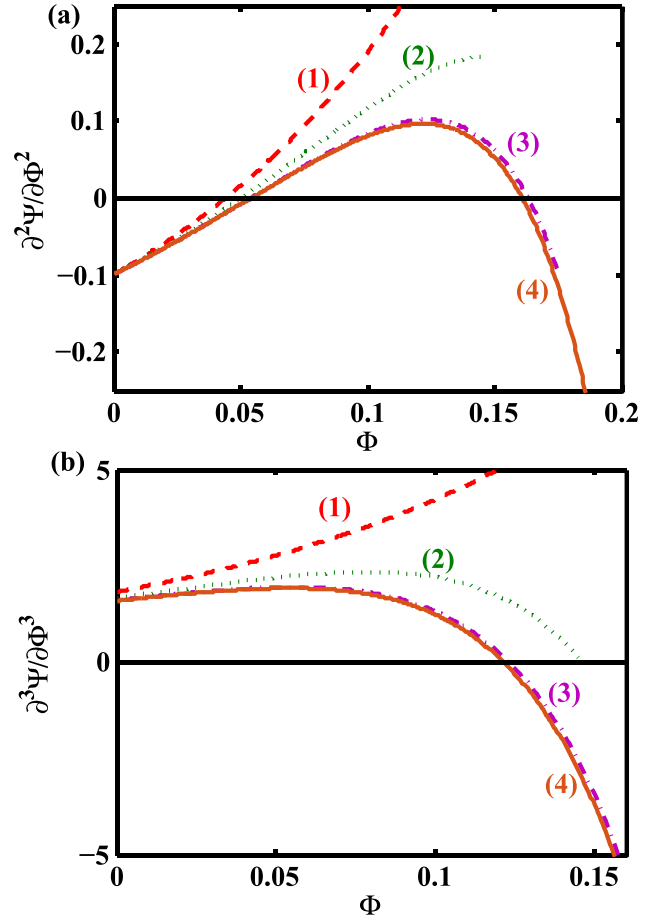
FIG. 3. (a) Variation of $\frac{\partial^2 \Psi}{\partial \Phi^2}$ Vs Φ and (b) $\frac{\partial^3 \Psi}{\partial \Phi^3}$ vs Φ; curves (1) and (2) RSW, (3) transitional RSW, and (4) DL.

represent RSWs, we have analyzed the higher order derivatives of the pseudopotential profiles. In Figs. 3(a) and 3(b), we have plotted the subsequent 2nd [Eq. (8)] and 3rd [Eq. (9)] order derivatives of the pseudopotential, respectively, while all the legends remain the same as earlier. The difference between the two groups of the solutions becomes readily evident as the subsequent roots of the corresponding $\frac{\partial^2 \Psi}{\partial \Phi^2}$ profiles differ. In Fig. 3(a), curves 3–4 show a non-monotonic variation for $\frac{\partial^2 \Psi}{\partial \Phi^2}$ Vs Φ with two roots, while for curves 1–2, the variation is monotonic with only one root. Between curves 1 and 4, it is well evident that the monotonic variation of the 2nd derivative gradually reaches up to the non-monotonic variation of curve 4 corresponding to a DL through curve 3. We may well argue that the RSWs associated with curves 1–3 represent a "degenerate state" of solutions which have two distinct kinds of derivative profiles, though they do not differ by their pseudopotentials. We may further conjecture that curve 3 is associated with a transitional region where the solution, being an RSW, has started incorporating some of the characteristics of a DL.

Our argument get further clarified in Fig. 3(b) where, expectedly, the 3rd order derivative profiles for curves 3–4 move from positive side to negative, having one root each, but for curves 1–2 it remains always positive without any root. This defines a limiting value of $\mu = \mu_r$, μ_r being that maximum μ value which supports a positive $\frac{\partial^3 \Psi}{\partial \Phi^3}$ for the

solution throughout the range. Mathematically, the condition can be written as

$$\frac{\partial^3 \Psi}{\partial \Phi^3} > 0 \quad \text{for all } 0 \leq \Phi \leq \Phi_0, \text{ provided } \mu \leq \mu_r; \quad (12a)$$

$$\frac{\partial^3 \Psi}{\partial \Phi^3} < 0 \quad \text{for some } \Phi, 0 \leq \Phi \leq \Phi_0, \text{ provided } \mu > \mu_r. \quad (12b)$$

The estimated value of μ_r for the present case is 0.00038.

According to Varghese and Ghosh,[38] for an RSW, the 3rd derivative of the Sagdeev pseudopotential should always be positive, i.e., $\frac{\partial^3 \Psi}{\partial \Phi^3} > 0$. Our present analysis, however, reveals that while $\frac{\partial^3 \Psi}{\partial \Phi^3} > 0$ is a sufficient condition for an RSW, it is not necessary. A compressive RSW in the vicinity of the corresponding DL, like curve 3 in Fig. 1(c), will show a negative value, or, alternatively, a single root for the 3rd derivative ($\frac{\partial^3 \Psi}{\partial \Phi^3}$). Rather than its termination, the parameter μ_r thus recognizes the onset of the transitional phase of the RSW to its corresponding DL beyond that critical value. This calls for a further clarification of the physical significance of μ_r and its role in the RSW–DL transition. Rather than to be a general condition for an RSW, the additional parametric condition, proposed in Eq. (12b), may well be argued as just an artifact of the transformation process. In order to eradicate this dilemma, we proceed to analyze the respective potential and Electric field (E-field) profiles.

Recalling that the extra maxima of curve 3 in Fig. 2 indicates a dip in Δn near the maximum amplitude, in Figs. 4(a)–4(d), we have plotted the respective potential profiles (solid lines) and their associated $\Delta n = n_i - n_e$ (dashed lines) for the pseudopotential profiles in Figs. 1(a)–1(d). The generalized coordinate $\eta = x - Mt$ ensures the steady state solution for the Sagdeev pseudopotential. It shows the usual bell shaped potential profiles of the positive polarity, representing

a compressive RSW [Figs. 4(a)–4(c)], and the familiar step shaped, or kink type, positive potential profile for the compressive DL [Fig. 4(d)]. To preserve the symmetry, the origin $\eta = 0$ of Fig. 4(d) is now shifted to coincide the η at the minimum of the pseudopotential. For the first two cases, i.e., Figs. 4(a)–4(b), the Δn profiles, too, resemble the corresponding potential profiles and have a "peak" near the amplitude, indicating a compression in the positive ion density. For Fig. 4(c), however, instead of a "peak" there appears a "trough" at the amplitude showing a dip in the charge separation. The "trough" gradually goes deeper, indicating a further decrease in the positive ion density and/or increase in the electron density. Eventually, the charge separation vanishes at the maximum amplitude and Δn illustrates the typical, fully grown bipolar structure for the DL [Fig. 4(d)]. Even though there are variations in the structure of Δn in Figs. 4(a)–4(d), the amplitude of the potential profile remains always positive. As μ increases and the nonlinear structures approach to the DL, the sharpness of the peak of the potential profile associated with the solitary wave reduces and seems to get more stretched out with the increasing amplitude (Φ_0).

To complement Figs. 4(a)–4(d), we have plotted the corresponding E-field profiles in Figs. 5(a)–5(d), respectively, which subsequently represent the RSWs {Figs. 5(a)–5(c), and the DL [Fig. 5(d)]}. The E-field profiles correspond to RSWs are bipolar in nature [Figs. 5(a)–5(c)], whereas that corresponds to the DL is monopolar [Fig. 5(d)].

Even though the derivatives of the RSW, represented in Fig. 1(c), behave differently from those in Figs. 1(a)–1(b), they all have the same bell shaped potential profiles and bipolar E-field structures which are the hallmark of an RSW. The bipolar electric field structures in Figs. 5(a)–5(c) ascertain that there is no discrepancy in their physical solutions which was also expected from their respective pseudopotential profiles [Figs. 5(a)–5(c)]. On the other hand, Figs. 2–4 clearly indicate a change in their internal physical processes
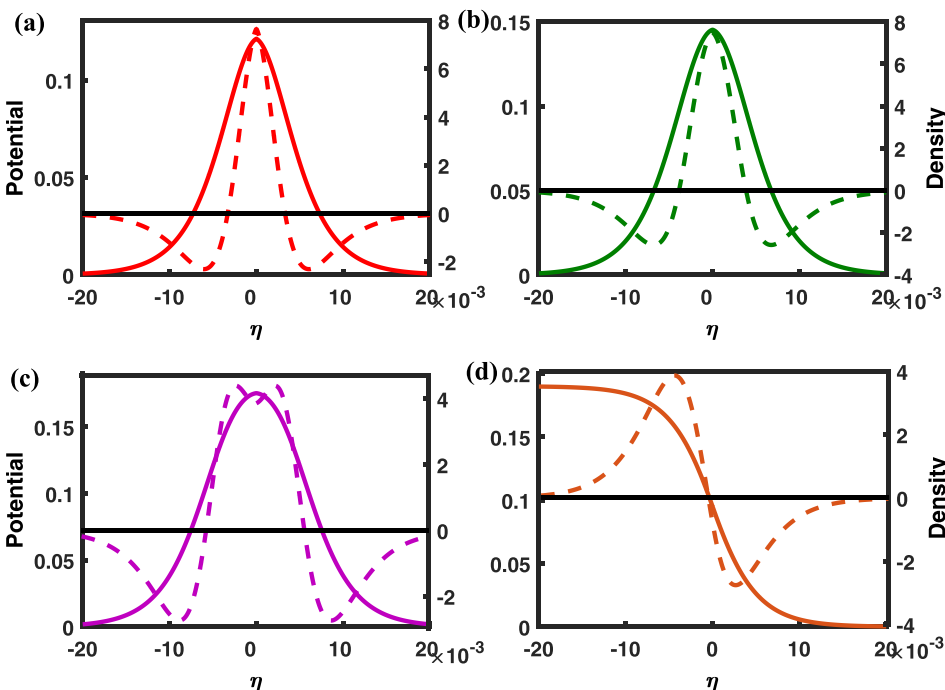
FIG. 4. Potential and Δn profiles for SWs and DL; (a) and (b) RSW, (c) transitional RSW, and (d) DL.
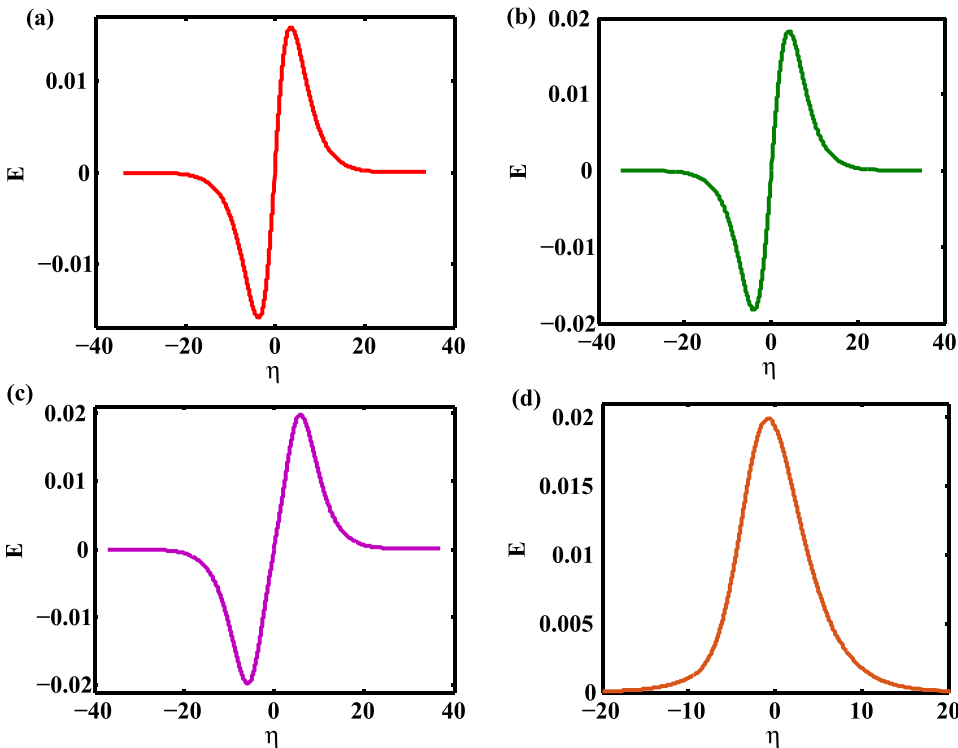
FIG. 5. Electric Field profile for SWs and DL; (a) and (b) RSW, (c) transitional RSW, and (d) DL.

which appears self-consistently with the increase in the minority component of the cooler electrons beyond its critical value (i.e., $\mu \geq \mu_r$). It is this change in the internal physical processes which appears to be correlated with, and hence possibly caused, the transformation of a compressive SW to its corresponding DL. We have reached this proposition because of the inherent correlation between μ_r and the fluctuation in the charge separation near the maximum amplitude. This correlation is attributed trivially to its definition [Eqs. 12(a) and 12(b)] on the basis of the derivative analysis. To ascertain our proposition, we need to find a more generic way to verify the physical significance of μ_r which should preferably be independent of any particular formalism associated with its derivation. It was previously noted that the width-amplitude variation of the solitary wave, too, may show a certain kind of degeneracy. Here, we have chosen to explore the role of μ_r, if any, on the overall width-amplitude variation profiles of the compressive IASWs. We have specifically focused on those IASW solutions which are going to be terminated as DLs. The subsequent results have been presented and discussed in Sec. III B.

B. Width amplitude analysis

According to the standard mathematical formalism, it is well known that the larger is the amplitude, the narrower becomes the soliton pulse. In other words, the width of a soliton is inversely proportional to its amplitude. This particularly holds true for a soliton derived from the Kortewege-de Vries (K-dV) equation, the celebrated nonlinear partial differential equation governing soliton solutions, or some other equations alike. The foremost hint of this width-amplitude relation was given by Zabusky and Kruskal[42] in their work on the nonlinear interaction of SW pulses in a dispersive

media. Later Washimi and Taniuti[43] validated the same as they derived the soliton solution analytically for a plasma system governed by the K-dV equation. Following them, others assumed it as one of the fundamental characteristics of K-dV solitons and also incorporated it to validate their experimental observations.[44,45] Ghosh and Iyengar,[46] however, contradicted the popular notion by presenting what they termed as the "anomalous width variation" where the width of the SW actually increases with the increasing amplitude. They have shown that, for a rarefactive (negative amplitude) IASW, the complete width-amplitude profile is not linear as expected from a K-dV like solution, but shows the shape of an "asymmetric parabola." For a small amplitude limit, they recovered the K-dV like pattern, which they called as Region I, while for a large amplitude (i.e., Region III according to their nomenclature), it shows an opposite trend leading to a DL. They showed that the particular trend is fairly consistent[47,48] and also applicable to space observations.[49,50]

From the above analyses it was inferred that, for a large amplitude rarefactive IASW, the solution shows a non-K-dV like, or "anomalous," width variation where the width increases with the increasing amplitude. In contrast, a compressive IASW, being of a small amplitude solution, follows a K-dV like variation, i.e., the width decreases with the amplitude. Recently, Ghosh and Iyengar[37] have shown that, prior to the occurrence of a compressive DL, the corresponding solitary wave do undergo an anomalous width variation even though it has a reasonably small amplitude. This also indicates that, rather than the external size of the nonlinear structure, it is the limiting solution associated with the structure which determines the width-amplitude variation pattern. In other words, irrespective of its amplitude, an anomalous width variation seems to always lead to a DL as its limiting

solution. Recalling our previous analyses, we may infer that the intricate internal physical processes within the localized structure changes according to the parameter regime and determines the characteristics, or phases of the particular nonlinear solution.[37] This phase is further determined by the particular limiting solution which provides the clue to the changes in the internal microphysics and manifests itself through the width-amplitude variation. This calls for a complete revisit of the width-amplitude variation processes of a compressive ion acoustic solitary wave, encompassing all its relevant parameter regime, which is currently beyond the scope of the present work. Rather we choose to confine our analysis for the parameter regime relevant to our interest, i.e., Region B2 in Ref. 37. The results are as follows.

In order to get a complete picture regarding width-amplitude analysis, we have estimated the half width W at $\Phi = \Phi_0/2$ by integrating the energy equation [Eq. (6)] numerically. To establish the general trend, we have assumed two β values, viz., $\beta = 0.03$ and $\beta = 0.04$, while we choose μ to be the dummy variable for changing the amplitude. To prevail adequate accuracy, we have chosen a higher resolution of μ (viz., $\delta\mu \approx 10^{-4}$) compared to other existing studies. All other parameters, viz., M, Q, σ, and α_l, remain constant. In Fig. 6, we have plotted W Vs. Φ_0 which readily confirms that, throughout the regime, the width has no decreasing trend, i.e., the solution is a non-K-dV one. Subsequently, the shape of the curve depicting $W - \Phi_0$ variation profile does not resemble any "asymmetric parabola" either, as obtained previously for rarefactive solitary waves.[46,47] The present variation pattern consists of two distinct segments, both showing a monotonic increase in W with increasing Φ_0 but their rate of increase is not uniform. Upto $\mu = \mu_r$, marked by the "○" in Fig. 6, it increases only marginally, but after that there is a significant increase in W with Φ_0. For the lower β value, the overall regime shifts to a smaller amplitude but the transitional trend continues. In order to understand the particular variation pattern, we have estimated the slopes of the $W - \Phi_0$ curves $\left(\frac{dW}{d\Phi_0}\right)$ and plotted them in Fig. 7 for the corresponding Φ_0 values. It readily
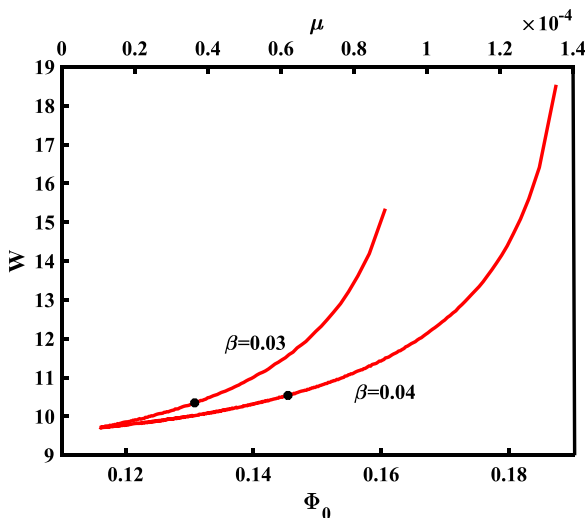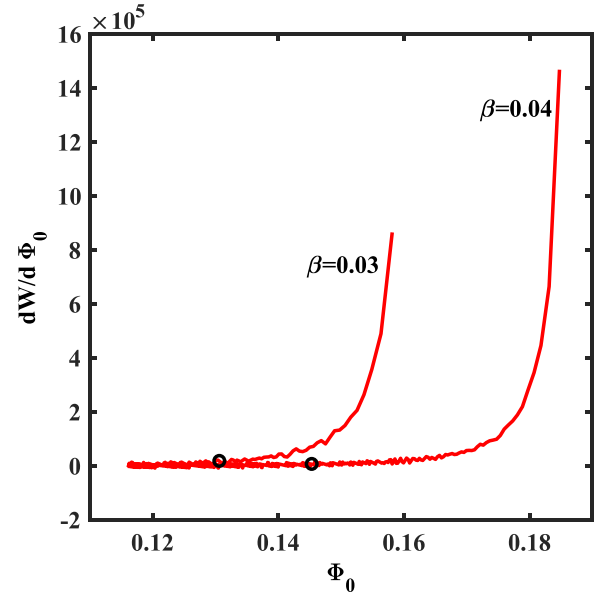
FIG. 7. Variation of slope of the $W - \Phi_0$ with Φ_0.

shows that, up to μ_r, $dW/d\Phi_0$ remains almost constant and almost near to zero, indicating a linear variation with a comparatively very small and marginal increase in the width. Significantly, just beyond μ_r, the slope $dW/d\Phi_0$ starts increasing with μ and Φ_0, showing a prominent increase in the width with increasing amplitude. This is followed by an ever increasing rate by which the associated nonlinear structure starts to expand. The expansion is evident from Figs. 6 and 7, and more specifically by the very sharp increase in the slope shown in the latter. Near the vicinity of the DL, the slope abruptly shoots up, resembling the "jump condition" prior to a "variable solitary wave" as discussed in Ref. 38. The trend further confirms that the solution beyond μ_r belongs to a transitional phase.

In Sec. III A, we have defined μ_r as that critical value of μ which determines the onset of the negative value, or, alternatively, a single root, for the 3rd derivative of the pseudopotential. We have found that the parameter trivially indicates a drop in the charge separation at the maximum amplitude. In the present section, we have tried to explore the influence of μ_r, if any, on the associated width-amplitude variation. We have found that there is a significant correlation between this critical parameter and the stretching of the nonlinear structure (i.e., increase in the width) with increasing amplitude. We have explored different β values which validates the consistency of our results. Combining these two results we may judiciously conclude that the critical parameter μ_r indeed play a deterministic role in the transition of a compressive ion acoustic solitary wave to a compressive DL. The inference holds true for the Region B_2 (i.e., low β − low μ) in Ref. 37 and is expected to hold true for other more general class of models as well.

In order to conserve the overall flux of the respective charged particles, the hotter electrons are accelerated through the positive amplitude profile and rarefied, while the positive ions get decelerated and further compressed. To interpret the role of μ_r, we may conjecture that, beyond certain critical

FIG. 6. Variation of W with Φ_0 with μ.

TABLE I. Plasma parameters estimated and as well as obtained from observation.

| Plasma parameters assumed | Observational parameters | Plasma scales | | |
		Assumed parameters	Estimated theoretically	Observational
$\beta = 0.031$	$T_e \approx 0.5 - 5\,\mathrm{eV}$	$T_{eff} = 5\,\mathrm{eV}$	$\lambda_d = 7.4339\,\mathrm{m}$	$\lambda_d \approx 5\,\mathrm{m}$
$\mu = 1.585 \times 10^{-3}$	$n_0 = 5 - 10\,\mathrm{cm}^{-3}$	$n_0 = 5\,\mathrm{cm}^{-3}$	$c_{isl} = 21.885\,\mathrm{km/s}$	
$\sigma = 0.033$				
$Q = 0.25$				
$M = 1.06$				

value of μ (i.e., μ_r), an additional increase in the minority component of the cooler electrons may start pulling out some of the positive ions away from the maximum amplitude resulting in a dip in the charge separation. This in turn stretches out the potential profile, eventually turning it to a DL. Alternatively, one may also claim that there is an increase in the possibility of trapping of cooler electrons within the positive structure for $\mu > \mu_r$. Such a scenario, however, is beyond the scope of our current fluid model and needs to be complemented by an adequate kinetic formalism.

C. Comparison with observational evidences

Satellite observations of low frequency, slow moving bipolar and monopolar electric pulses were often interpreted as IASWs or DLs. These observations consistently showed that a taller pulse is wider too, i.e., the width increases with the increasing amplitude. This contradicts the usual notion of a solitary wave whose width is expected to decrease when the amplitude increases. In Sec. III B, we have already pointed out the "anomalous width variation" for the large amplitude rarefactive (negative polarity) ion acoustic solitary waves which befit the trend of the satellite observations. In situ measurements generally find it difficult to determine the polarity of the observed structures, though theoretically they were often interpreted as a negative amplitude solution. However, the possibility of the existence of positive polarity structures cannot be ruled out. As early as the first observation by S3–3 satellite, Temerin et al.[7] indicated the presence of positive polarity structures in the auroral region (Sec. I). In Sec. III B, we have confirmed "anomalous width variation" for a positive amplitude solution as well. This indicates that the present plasma model can be implemented to study the signatures of the positive amplitude DL (monopolar structures) in the auroral acceleration region. To validate our results with space plasma observations, we have compared our theoretical estimations with the S3-3 satellite

observation. The results are summarized in Tables I and II as described below.

The observational data presented by Temerin et al.[7] in the auroral acceleration region reports the electron temperature ranging from 0.5 to 5 eV, and the electron densities ranging from 5 to 10 cm^{-3} at the height of approximately 8000 km. In accordance with those observed parameters, we have assumed T_{eff} ($\approx T_e$) = 5 eV and $n_0 = 5$ cm^{-3}. From these inputs we have estimated the scales of our plasma model, viz., the Debye length λ_d (=7.4339 m), the ion acoustic speed c_{isl} (=21.885 km/s), and the proton plasma frequency ($\omega_p = 2.9439$ kHz), which were found to be consistent with the satellite observations. Table I has enlisted both the observed and the assumed plasma parameters as well as the corresponding estimations of the relevant plasma scales.

For an electron temperature ratio $\beta = 0.031$ and a cooler electron concentration $\mu = 1.585 \times 10^{-3}$, as mentioned in Table I, our plasma model supports a compressive ion acoustic DL, moving with the Mach number $M = 1.06$. The normalized amplitude Φ_d (= 0.1679) has been obtained from the Sagdeev pseudopotential, while the normalized width W (=11.9306) has been obtained by integrating Eq. (6) numerically. In order to compare with the satellite observations, we have converted our results to the corresponding non-normalized values by incorporating appropriate normalization parameters (Table I). Remembering that the "pseudoparticle" does not reflect or retrace itself back from Φ_d [Eq. (11)], we redefined the width of the DL as

$$W = \eta_{1/2} = \int_{\frac{\Phi_0}{2}}^{\Phi_0} \left(\frac{1}{\sqrt{(-2\Psi(\Phi))}} \right) d\Phi. \qquad (13)$$

The associated time duration (Δt) has been obtained from W assuming $x = 0$ for the generalized coordinate η ($= x - Mt$), i.e.,

$$\Delta t = \left(\frac{W}{M} \right)', \qquad (14)$$

where the prime denotes the non-normalized quantity. To estimate the associated average E-field, we have assumed

$$E_{avg} = \frac{\Phi_d'}{W'} \qquad (15)$$

while the maximum E-field is estimated as

TABLE II. Wave parameters.

| Theoretical | | |
Normalized	Non-normalized	Observational
$\Phi_0 = 0.1679$	$E_{avg} = 9.4683\,\mathrm{mV/m}$	$E \leq 15\,\mathrm{mV/m}$
	$E_{max} = 13.3847\,\mathrm{mV/m}$	
$W = 11.9306$	$\Delta t = 3.8232\,\mathrm{ms}$	$\Delta t = 2 - 20\,\mathrm{ms}$
	$V = 23.198\,\mathrm{km/s}$	$V \approx 50\,\mathrm{km/s}$
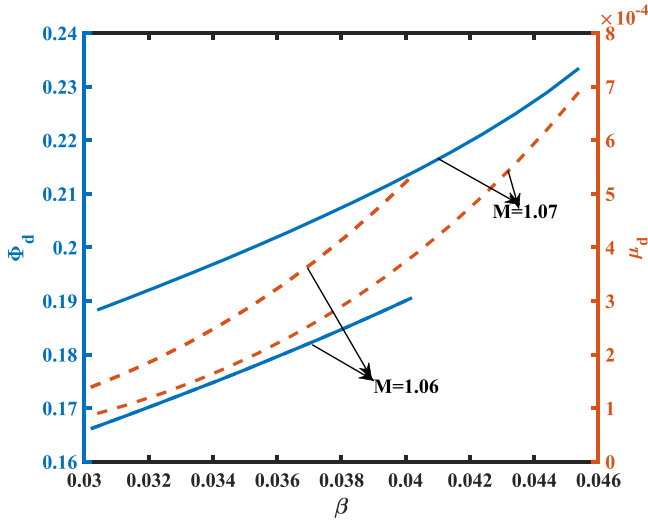
FIG. 8. Variation of μ_d and Φ_d with β.

$$E_{max} = -\left(\frac{d\Phi}{d\eta}\right)'\bigg|_{\Psi=\Psi_{min}}, \qquad (16)$$

where $d\Phi/d\eta$ has been obtained from Eq. (6) at the minimum value of Ψ. Table II compares our analytical estimations of the shape, size, and velocity of the DL with the observations. It shows that our theoretical estimations are well within the range of the satellite observations. This further validates that our model is appropriate for interpreting the satellite observations and may further be applicable for understanding the observed nonlinear wave phenomena in space plasmas.

D. Existence domain

To complete our discussion, here we have delineated the existence domains of the RSW and the DL. In Fig. 8, we have plotted the variation of Φ_d (solid lines) and the corresponding μ_d (dashed lines) with β for two different Mach numbers, viz., 1.06 and 1.07. It shows that the amplitude of
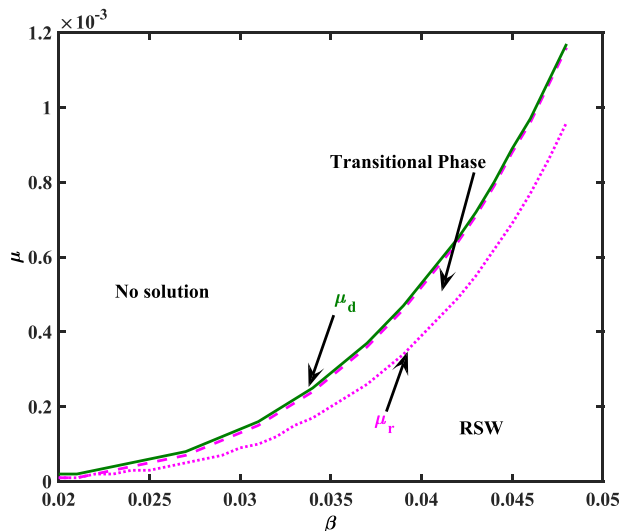
FIG. 9. Regime of SWs and DLs.

the DL (Φ_d) increases both with β and M. As β increases, the corresponding μ_d also increases, but for a larger M, it drops significantly. As M increased, the extent of the β value supporting the DL also increases to a good extent.

To find their existence domains, it is necessary to determine the characteristic μ values which marks the onset and offset of different nonlinear structures. During the process of the transition of an RSW to a DL, we have found two characteristic μ values, viz., "μ_r" and "μ_d" where the former characterizes the initialization of the transitional process and the latter is associated with the DL. We have observed that all these characteristic μ values varies significantly with varying β which in turn affects the parameter regime of the nonlinear structures. In Fig. 9, we have plotted the variation of μ_r (dotted line) and μ_d (solid line) with β. The region between the μ_r and μ_d represents the transitional phase between an RSW and DL. The region below μ_r represents those RSWs which are not affected by the limiting solution. The complete existence domain of the RSW, however, is bounded below μ_d, shown by the dashed line in Fig. 9.

IV. CONCLUSION

In the present paper, we have delineated the transition of a compressive IASW to its corresponding DL. The plasma parameters supporting a compressive DL belong to a low β-low μ regime (Region B2 in Ref. 37) which is associated with the lower end of the "forbidden region" in μ. Using the derivative analysis, we have identified a critical value of μ ($=\mu_r$) which triggers the transitional phase of an RSW toward the corresponding DL solution. We have found that an RSW in this regime has a kind of "degeneracy" in their solution. Physically and qualitatively all RSW solutions are indistinguishable as all of them are associated with the typical bipolar electric field and the bell shaped potential profiles, and the morphology of their associated Sagdeev pseudopotential is also not distinguishable either. However, the microphysics within the localized potential structure differs significantly before and after the critical value of μ_r due to the change in the charge separation profile near the maximum amplitude. Instead of a peak, it shows a trough near Φ_0 as μ increases beyond μ_r. This further manifests itself in a rapid increase in the width with the amplitude, triggered after that critical value. The two processes, together, "stretch" the localized structure, ultimately converting it to a DL.

In the above analysis, we have defined μ_r as that maximum value of μ for which the 3rd derivative remains positive throughout the range of Φ. In our previous study, we introduced the same condition to distinguish an extra-nonlinear solution from the corresponding RSW. The present result reveals that the condition is though sufficient, but not necessary for an RSW. In other words, an RSW in its transitional phase will violate this condition but will remain physically indistinguishable from those RSW solutions which are in the non-transitional phase and satisfy the aforementioned condition. This calls for a more critical definition for the onset of an extra-nonlinear solution. A work in this direction is currently under progress and will be communicated shortly.

After identifying the transitional phase between the RSW and DL, we have delineated their respective existence domains. It confirms a "jump condition" where the amplitude shoots up abruptly to a large value as the solution approaches, or converts, to a DL. The abruptness or the "jump condition" resembles that observed previously during the onset of a variable solitary wave (VSW).[39] Though a DL is a well-studied structure and the concept of the VSW emerged only very recently, the salient features of their respective transitional patterns appear to be fairly analogous and may need further comparative studies.

It has been confirmed that the parameter regime of our concern governs only a non-K-dV like solution which shows an anomalous increase in the width with the amplitude. This motivated us to compare our results with the satellite observations of Temerin *et al.*[7] It shows a good agreement. This further validates our model for its applicability to interpret the slowly moving ESWs in the auroral region.

ACKNOWLEDGMENTS

[1]H. Matsumoto, H. Kojima, T. Miyatake, Y. Omura, M. Okada, I. Nagano, and M. Tsutsu, Geophys. Res. Lett. **21**, 2915–2918, https://doi.org/10.1029/94GL01284 (1994).

[2]H. Matsumoto, H. Kojima, Y. Kasaba, T. Miyake, R. R. Anderson, and T. Mukai, Adv. Space Res. **20**, 683–693 (1997).

[3]J. S. Pickett, L.-J. Chen, S. W. Kahler, O. Santolík, D. A. Gurnett, B. T. Tsurutani, and A. Balogh, Ann. Geophys. **22**, 2515–2523 (2004).

[4]C. Cattell, J. Crumley, J. Dombeck, R. Lysak, C. Kletzing, W. K. Peterson, and H. Collin, Adv. Space Res. **28**, 1631–1641 (2001).

[5]W. Lotko and C. F. Kennel, J. Geophys. Res.: Space Phys. **88**, 381–394, https://doi.org/10.1029/JA088iA01p00381 (1983).

[6]H. Alfvén and P. Carlqvist, Sol. Phys. **1**, 220–228 (1967).

[7]M. Temerin, K. Cerny, W. Lotko, and F. S. Mozer, Phys. Rev. Lett. **48**, 1175–1179 (1982).

[8]R. E. Ergun, L. Andersson, J. Tao, V. Angelopoulos, J. Bonnell, J. P. McFadden, D. E. Larson, S. Eriksson, T. Johansson, C. M. Cully, D. N. Newman, M. V. Goldman, A. Roux, O. LeContel, K.-H. Glassmeier, and W. Baumjohann, Phys. Rev. Lett. **102**, 155002 (2009).

[9]A. Mangeney, C. Salem, C. Lacombe, J.-L. Bougeret, C. Perche, R. Manning, P. J. Kellogg, K. Goetz, S. J. Monson, and J.-M. Bosqued, Ann. Geophys. **17**, 307–320 (1999).

[10]S. D. Bale and F. S. Mozer, Phys. Rev. Lett. **98**, 205001 (2007).

[11]F. S. Mozer, S. D. Bale, J. W. Bonnell, C. C. Chaston, I. Roth, and J. Wygant, Phys. Rev. Lett. **111**, 235002 (2013).

[12]F. S. Mozer and A. Hull, J. Geophys. Res.: Space Phys. **106**, 5763–5778, https://doi.org/10.1029/2000JA900117 (2001).

[13]R. E. Ergun, L. Andersson, D. S. Main, Y.-J. Su, C. W. Carlson, J. P. McFadden, and F. S. Mozer, Phys. Plasmas **9**, 3685–3694 (2002).

[14]L. Andersson, R. E. Ergun, D. L. Newman, J. P. McFadden, C. W. Carlson, and Y.-J. Su, Phys. Plasmas **9**, 3600–3609 (2002).

[15]H. Schamel, Z. fr Naturforsch. A **38**, 1170–1183 (1983).

[16]K. Y. Kim, Phys. Fluids **30**, 3686–3694 (1987).

[17]F. W. Perkins and Y. C. Sun, Phys. Rev. Lett. **46**, 115–118 (1981).

[18]W. L. Theisen, R. T. Carpenter, and R. L. Merlino, Phys. Plasmas **1**, 1345–1348 (1994).

[19]S. L. Cartier and R. L. Merlino, Phys. Fluids **30**, 2549–2560 (1987).

[20]R. F. Hubbard and G. Joyce, J. Geophys. Res.: Space Phys. **84**, 4297–4304, https://doi.org/10.1029/JA084iA08p04297 (1979).

[21]J. S. Wagner, T. Tajima, J. R. Kan, J. N. Leboeuf, S. I. Akasofu, and J. M. Dawson, Phys. Rev. Lett. **45**, 803–806 (1980).

[22]R. A. Smith, Phys. Scr. **1982**, 238.

[23]T. Sato and H. Okuda, Phys. Rev. Lett. **44**, 740–743 (1980).

[24]H. Okuda and M. AshourAbdalla, Phys. Fluids **25**, 1564–1569 (1982).

[25]C. Barnes, M. K. Hudson, and W. Lotko, Phys. Fluids **28**, 1055–1062 (1985).

[26]P. C. Gray, M. K. Hudson, and W. Lotko, IEEE Trans. Plasma Sci. **20**, 745–755 (1992).

[27]K. S. Goswami and S. Bujarbarua, Phys. Lett. A **108**, 149–152 (1985).

[28]K. S. Goswami and S. Bujarbarua, J. Phys. Soc. Jpn. **56**, 2396–2400 (1987).

[29]S. G. Tagare, Phys. Plasmas **7**, 883–888 (2000).

[30]R. Roychoudhury and S. Bhattacharyya, J. Plasma Phys. **42**, 353–360 (1989).

[31]F. Verheest, T. Cattaert, M. A. Hellberg, and R. L. Mace, Phys. Plasmas **13**, 042301 (2006).

[32]R. H. Berman, T. H. Dupree, and D. J. Tetreault, Phys. Fluids **29**, 2860–2870 (1986).

[33]S. B. Bujarbarua and H. Schamel, J. Plasma Phys. **25**, 515–529 (1981).

[34]S. Baboolal, R. Bharuthram, and M. A. Hellberg, J. Plasma Phys. **44**, 1–23 (1990).

[35]M. Tribeche and N. Boubakour, Phys. Plasmas **16**, 084502 (2009).

[36]M. K. Mishra, R. S. Tiwari, and S. K. Jain, Phys. Rev. E **76**, 036401 (2007).

[37]S. S. Ghosh and A. N. Sekar Iyengar, Phys. Plasmas **21**, 082104 (2014).

[38]S. S. Varghese and S. S. Ghosh, Phys. Plasmas **23**, 082304 (2016).

[39]S. V. Steffy and S. S. Ghosh, Phys. Plasmas **24**, 102111 (2017).

[40]P. H. Sakanaka, Phys. Fluids **15**, 304–310 (1972).

[41]R. B. White, B. D. Fried, and F. V. Coroniti, Phys. Fluids **15**, 1484–1490 (1972).

[42]N. J. Zabusky and M. D. Kruskal, Phys. Rev. Lett. **15**, 240–243 (1965).

[43]H. Washimi and T. Taniuti, Phys. Rev. Lett. **17**, 996–998 (1966).

[44]H. Ikezi, Phys. Fluids **16**, 1668–1675 (1973).

[45]Y. Nakamura and A. Sarma, Phys. Plasmas **8**, 3921–3926 (2001).

[46]S. S. Ghosh, K. K. Ghosh, and A. N. Sekar Iyengar, Phys. Plasmas **3**, 3939–3946 (1996).

[47]S. S. Ghosh and A. N. Sekar Iyengar, Phys. Plasmas **4**, 3204–3210 (1997).

[48]S. S. Ghosh and A. N. Sekar Iyengar, J. Plasma Phys. **67**, 223–233 (2002).

[49]J. Dombeck, C. Cattell, J. Crumley, W. K. Peterson, H. L. Collin, and C. Kletzing, J. Geophys. Res.: Space Phys. **106**, 19013–19021, https://doi.org/10.1029/2000JA000355 (2001).

[50]S. S. Ghosh and G. S. Lakhina, Nonlinear Process. Geophys. **11**, 219–228 (2004).